Heat-Transfer Prediction in the Riser of a Novel Fluidized Catalytic Cracking Unit

ARTICLE *in* INDUSTRIAL & ENGINEERING CHEMISTRY RESEARCH · SEPTEMBER 2001

Impact Factor: 2.59 · DOI: 10.1021/ie0008777

4 AUTHORS, INCLUDING:

H. De Lasa
The University of Western Ontario
239 PUBLICATIONS **3,488** CITATIONS

SEE PROFILE

Heat-Transfer Prediction in the Riser of a Novel Fluidized Catalytic Cracking Unit

A. Blasetti[†] and H. de Lasa*[,‡]

Bolland y Cía., Macizo 6 Parque Industrial, Comodoro Rivadavia, Chubut, Argentina, and Chemical Reaction Engineering Centre, The University of Western Ontario, London, Ontario, Canada N6A 5B9

The present study considers a "Multicrackex" unit constituted by a riser reactor with an upflow catalyst suspension exchanging heat with a surrounding fluidized-bed regenerator. A statistical-based analysis is developed to establish a semiempirical correlation able to describe the heat transport phenomena between a bundle of riser reactor tubes and a fluidized-bed regenerator. The proposed correlation is tested and developed under reaction and realistic conditions for fluidized catalytic cracking (FCC) units, and this adds special value to the study developed. In this respect, the present study provides data that may be of particular interest for the design of novel FCC processes.

1. Introduction

Riser reactors are frequently used in the petrochemical industry for the catalytic cracking of gas oil. In riser reactors, a gas-phase reactant mixture lifts a dilute catalyst suspension. These units are frequently operated in an adiabatic or a close to adiabatic mode.

The concept of a novel fluidized catalytic cracking (FCC) unit, the so-called Multicrackex unit of the present study, is based on an upflow catalytic reactor (riser) exchanging heat with a surrounding dense fluidized bed. More specifically, in the context of the FCC process, the dense fluidized bed is constituted by a bed of hot catalyst particles (regenerator). This bed contains a bundle of vertical riser reactor tubes where the endothermic catalytic cracking reaction is taking place.[1,2]

Farbar and Morley[3] studied heat transfer in flowing suspensions. Experimental information was obtained with air and FCC cracking catalyst flowing in a 0.0175 m i.d. and a 0.84 m long tube. The derived correlation (Table 1) assumes that heat is transferred from the walls of the tube through the gas boundary layer. Heat transfer by radiation from the tube walls to the gas−solid suspension and by conduction from the walls to solid particles is neglected.

Wen and Miller[4] developed an empirical correlation for either vertical or horizontal transport lines (Table 1). This correlation, also applicable to the dilute phase of fluidized beds, satisfactorily represents the data of Farbar and Morley.[3] Because the physical properties of the gas are evaluated at the temperature of the film, this correlation was considered suitable for both cooling and heating conditions. It is reported, however, that Wen and Miller's correlation is not suitable for data obtained by Danziger,[5] who correlated data from Kellogg's units and Farbar and Morley[3] with *Nu* and *Re* dimensional numbers based on the tube internal diameter (Table 1).

Rao and Murti[6] correlated heat transfer to gas−solid suspensions in vertical tubes. These authors found that the particle property, gas superficial velocity, and solid loading influence the heat-transfer coefficients (Table 1). Among other materials, these authors used silica−alumina ($d_p = 47\ \mu$m) and sand particles.

Correlations for flowing gas−solid suspensions developed with solid particles other than FCC catalyst or silica−alumina catalysts are available in the technical literature.[7−11] Experimental heat-transfer coefficients using 269−109 μm glass beads were also reported using Sadek's correlation[12] by Lunardelli-Furchi et al.[13]

There are as well a number of theoretical models to represent the heat-transfer process in gas−solid flowing suspensions. A theoretical approach[14] based on the use of probabilistic multiphase flow equations for vertically flowing gas−solid suspensions was implemented by Bentahar et al.[15] An alternative theoretical analysis[16] considers momentum balances, heat balances, and a mixing length parameter. It was found that this approach represents the experimental heat-transfer coefficients for gas−solid suspensions in vertical pipes and in particular the data of Farbar and Morley.[3]

While there have been valuable studies on heat-transfer phenomena in gas−solid suspensions, there is limited information about heat-transfer data under reaction conditions for FCC. Thus, the present study provides data of particular value for the design of novel FCC units.

2. Experimental Setup

Figure 1 reports a schematic diagram of the experimental setup of the present study. The regenerator of the unit (R-101) had an outside diameter of 0.266 m and a height of 3.25 m. The riser (R-201) had an outside diameter of 0.0344 m and a total height of 3.46 m. Both the regenerator and the riser tubes were made out of Inconel 601. Air, fed into the regenerator, was evenly distributed by using a perforated grid.[1] The unit was designed for operating conditions up to 179 kPa, regenerator temperatures of about 730 °C, and catalyst-to-oil ratios in the riser between 1 and 12. The total height of the dense-phase fluidized-bed regenerator was usually maintained between 1.3 and 1.6 m.

Figure 2 displays a top view of the unit and provides details of the three Inconel-601 pipes simulating a triangular array of a bundle of tubes in a heat ex-

* Corresponding author. E-mail: Hdelasa@eng.uwo.ca.
[†] Comodoro Rivadavia.
[‡] The University of Western Ontario.

10.1021/ie0008777 CCC: $20.00
Published on Web 09/20/2001

Table 1. Heat-Transfer Correlations for FCC Catalyst in Gas−Solid Suspensions

ref	heat-transfer correlation	application range
3	$\frac{h_{sus}d_t}{\lambda_g} = 0.14\left(\frac{d_t G_g}{\mu_g}\right)^{0.6}\left(\frac{G_p}{G_g}\right)^{0.45}$	$d_t = 0.017\ 78$ m, $10 < d_p < 210\ \mu$m, $1.3 \times 10^4 < Re < 2.8 \times 10^4$, $2 < G_p/G_g < 13.3$
4	$h_{sus} = \left(\frac{C_{ps}\mu_g}{d_p}\right)\left(\frac{\rho_{mix}}{\rho_p}\right)^{0.3}\left(\frac{u_t^2}{g d_p}\right)^{0.21}$ where $\rho_{mix} = \frac{\left(\frac{G_p}{G_g}+1\right)\rho_p\rho_g}{\left(\frac{G_p}{G_g}\rho_g + \rho_p\right)}$	$1.8 < d_p < 450\ \mu$m, $0.18 < G_g < 188.5$ kg/(m^2·s), $1.18 < \rho_{mix} < 1121.4$ kg/m^3, $1361.7 < \rho_s < 2835.5$ kg/m^3
5	$\frac{h_{sus}d_t}{\lambda_g} = 0.0784\left(\frac{d_t G_g}{\mu_g}\right)^{0.66}\left(\frac{G_p}{G_g}\right)^{0.45}$	$178 < Re < 25\ 400$, $2 < G_p/G_p < 446$, $0.017 < d_t < 0.038$ m
6	$\frac{h_{sus}d_t}{\lambda_g} = 4.5 \times 10^{-3}\left(\frac{d_t G_g}{\mu_g}\right)^{0.66}\left(\frac{d_t}{d_p}\right)^{0.65}\left(\frac{u_t}{u_g}\right)^{0.3}\left(\frac{C_{ps}}{C_{pg}}\right)^{1.1}\left(\frac{G_p}{G_g}\right)^{0.42}$	$d_t = 0.019$ m, $d_p = 47\ \mu$m, $0 < G_p/G_g < 14$, $5.15 < u_g < 12.2$ m/s

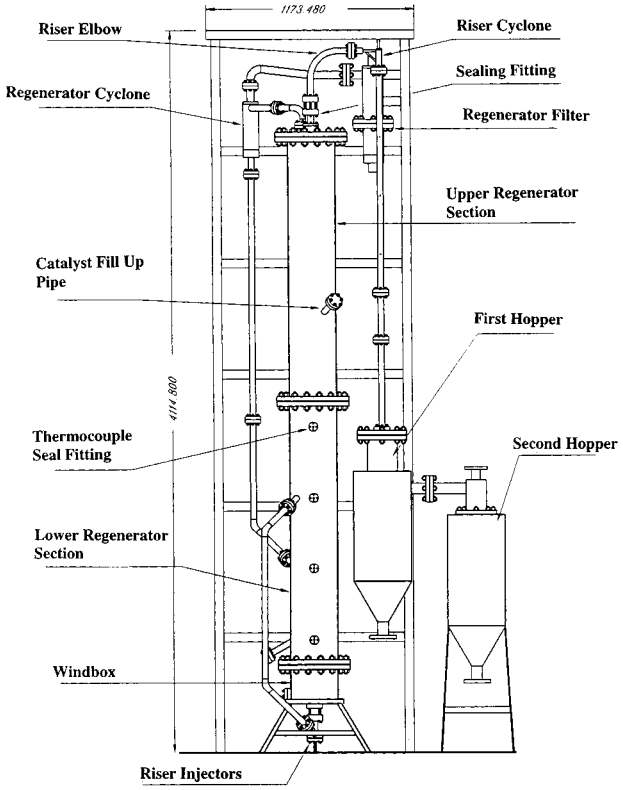

Figure 1. Schematic diagram of the experimental setup: (a) the regenerator of the unit (R-101); (b) the riser (R-201). Units of various dimensions in millimeters if omitted.

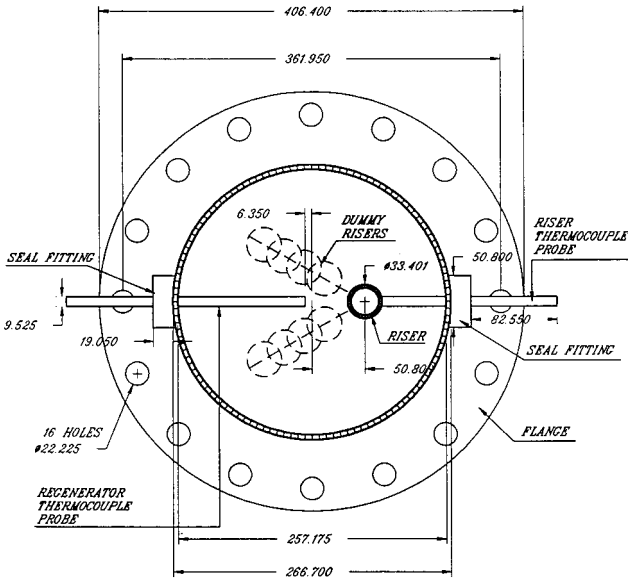

Figure 2. Top view of the triangular array of a bundle of tubes in a heat exchanger placed inside the regenerator. Catalytic cracking reactions take place in only one of these tubes (riser). This figure illustrates the positioning and shifting of the "dummy" risers. Units of various dimensions in millimeters if omitted.

changer. Catalytic cracking reactions took place in only one of these tubes (riser), while the other two tubes ("dummy" risers) were employed to provide a triangular geometry. A special design allowed shifting of the "dummy" risers to change the pitch between the riser tubes.

A 3 m height Plexiglas model of the riser reactor was built to simulate the operation of the unit and to assess proper operation. A homogeneous gas−solid flow pattern was observed in all cases with some solid recirculation noticed.[1] This solid recirculation took place at the higher axial positions, close to the tube walls, and for the highest solid flow rates. Choking velocities were calculated using Yang's equation[17] and were confirmed experimentally in the Plexiglas model.

Cracking experiments were carried out using a commercial catalyst (Akzo Octaboost 6XX series) and synthetic crude gas oil (CANMET SF-135). A pseudofactorial experimental design was adopted for the study.[18] Targeted factor levels were selected as reported in Table 2: (a) 580−730 °C for the temperature in the regenerator, (b) 1.5−5.5 s for the contact time, defined at riser entry conditions, and (c) 1−12 for the catalyst-to-oil ratio.

Table 2. Factor Levels Selected for the Experimental Program[1]

	regenerator temp (°C)	contact time at riser entry (s)	catalyst-to-oil ratio
(−) low range	580−610	1.5−2.5	1.0−3.5
(+) high range	700−730	4.5−5.5	7.0−12.0
(0) center range	640−670	3.0−4.0	5.0−7.0

Entrained solids from the regenerator were returned to the bed via a single-stage cyclone. At the end of the riser, a two-stage cyclone was used to separate the catalyst particles. Four thermocouples installed in the riser unit and six thermocouples in the regenerator vessel were connected to a data acquisition system and thermocouple amplifier/multiplexer (Cole-Parmer catalog nos. 8109-27 and 8109-02) to record temperature readings.

To ease the operation of the unit, the conveyed solids in the riser (spent catalyst) were not returned directly to the fluidized regenerator and were collected and measured in two hopper bins. The gaseous mixture of unconverted reactants and products was sent to a

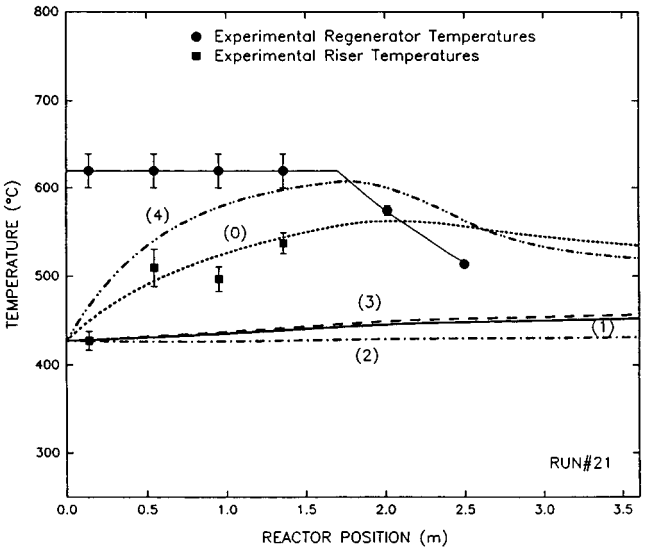

Figure 3. Temperature profiles in the riser and in the regenerator. (■) Experimental riser temperatures. (●) Experimental regenerator temperatures. (0) Temperature predictions using the heat-transfer correlation of this study and the data of Blasetti and de Lasa.[18] (1) Temperature predictions using Danziger's heat-transfer correlation[5] and the data of Blasetti and de Lasa.[18] (2) Temperature predictions using Rao and Murti's heat-transfer correlation[6] and the data of Blasetti and de Lasa.[18] (3) Temperature predictions using Farbar and Morley's heat-transfer correlation[3] and the data of Blasetti and de Lasa.[18] (4) Temperature predictions using Wen and Miller's heat-transfer correlation[4] and the data of Blasetti and de Lasa.[18]

condenser and a gas−liquid separator for further analysis. Catalyst was regenerated by coke combustion in the dense fluidized bed during separate runs.

Figure 3 illustrates the experimental temperature profiles both in the regenerator and in the riser of the Multicrackex unit. A progressive initial increase of the riser temperature was consistently observed with the riser height. The temperature in the dense phase of the regenerator remained, however, essentially constant up to 1.8 m height. From this axial position and on, the temperature in the regenerator steadily declined, with the temperature in the riser leveling off and decreasing afterward. These temperature profiles were the result of heat-transfer conditions prevalent in the regenerator, with the temperature kept at the desired value using electrical heaters placed at the dense bed section level and outside the unit. There was no heater placed on the Multicrackex unit outer walls at the freeboard section level.

Regarding measured suspension temperatures in the riser side of the unit, they represented average values between the gas and the particle temperatures. Placing temperature ports away from the feedstock injection point minimized the influence of entry effects on temperature readings. The closet measurement port was placed at a distance of more than 10 times the pipe diameter.

Additional details about the setup and the experimental techniques of the present study are reported in ref 1.

3. Modeling Heat-Transfer Phenomena: Regenerator Side

Operating conditions may affect the heat-transfer process from fluidized beds to immersed heating or cooling surfaces. As a result of this, different mechanisms can be proposed for its representation. In addition, fluid dynamic conditions may change as one moves from the dense phase to the dilute phase (freeboard), and as a result, different calculation procedures should be implemented for each zone.

For a dense-phase fluidized-bed regenerator, it is widely accepted that the overall heat-transfer coefficient, the so-called bed film coefficient (h_{reg}), can be represented as the sum of the following contributions: (1) a particle convective component (h_{pc}); (2) an interphase gas convective component (h_{gc}); (3) a radiant component of the heat transfer (h_r).[19−24] For small particles (FCC type), it has been consistently reported that the gas convective contribution is not significant and can be disregarded.[25−28] Therefore, the regenerator-side heat-transfer coefficient can be evaluated as

$$h_{reg} = h_{pc} + h_r \qquad (1)$$

The first term of eq 1 considers the molecular heat conduction through the gas layer between the wall and the closest row of particles, and the second term accounts for the radiant heat transfer occurring between the surface and the "visible" particles. It has been reported that radiation may become important for beds operating at high temperatures, usually above 800 K.[21]

Regarding the particle convective component, Ackeskog et al.[29] showed that its influence is considerable for small particles (e.g., 40−800 μm), as in the case of Geldart's powders of types A and B. There are several models and correlations proposed to represent this component.[21−23,30−34] For instance, Molerus[35] proposed a laminar flow model and uses the Archimedes number to define the fluid dynamics of the system. This analysis is based on the two-phase theory of fluidization, with the emulsion phase at minimum fluidization conditions.[35] Other empirical equations, such as the one introduced by Zabrodsky,[36] are helpful for practical purposes, given that it yields an upper value for the heat-transfer coefficient and has been cited as the one giving the best predictions.[35,37] Another alternative equation to evaluate the regenerator-side film transfer coefficient is the one proposed by Gelperin and Einstein.[38] This equation is reported as being valuable, for bundles of spaced vertical tubes, immersed in a fluidized bed.

On the other hand and considering the temperature levels of this study, the radiative component on the film coefficient for the regenerator has to be included. A possible approach for the radiant component of the heat-transfer coefficient is based on the use of the Stefan−Boltzmann's equation.[29,38−40] Although it may be argued that this approach may not be fully adequate, the use of Stefan−Boltzmann's equation is frequently selected.[40−42]

In the context of the present study, there is the need of suitable heat-transfer correlations for the regenerator freeboard region. Subbarao and Basu[43] considered the transient conduction of heat to a stagnant film located between clusters. It has been reported that this model leads to low heat-transfer coefficients.[42] Hashimoto et al.[44] proposed a correlation to evaluate the heat-transfer coefficient of vertical tubes in the freeboard of a turbulent fluidized bed. Nevertheless, its use is questionable given that such a correlation does not include the particle concentration in the dilute phase, considered to play an important role on heat transfer in the

freeboard region of a fluidized bed. Given the facts described, an empirical correlation advanced by Wen and Miller[4] was considered for further modeling

$$h_{sus} = \left(\frac{C_{ps}\mu_g}{d_p}\right)\left(\frac{\rho_{mix}}{\rho_p}\right)^{0.3}\left(\frac{u_t^2}{gd_p}\right)^{0.21}; \quad \rho_{mix} = \frac{\left(\frac{G_p}{G_g}+1\right)\rho_p\rho_g}{\left(\frac{G_p}{G_g}\rho_g+\rho_p\right)} \tag{2}$$

Particle entertainment calculations in the freeboard were considered with the following expression:[45]

$$G_p = \sum K_{i,\infty}; \quad K_{i,\infty} = C_1\mu_g U_{gas}\left(\frac{u_g}{gd_{pi}\rho_p^2}\right) \tag{3}$$

with $C_1 = 1.26 \times 10^7$ for $(u_g/gd_{pi}\rho_p^2) < 3 \times 10^4$ and $C_1 = 4.31 \times 10^4$ for $(u_g/gd_{pi}\rho_p^2) > 3 \times 10^4$ and $K_{i,\infty}$ representing the elutriation rate constant for d_{pi}, the size fraction at an axial position in the freeboard bigger than TDH (transport disengagement height).

This correlation gives realistic results for elutriation of particles smaller than 100 μm, as in the case of a catalytic cracking catalyst, from fluidized beds operated at up to 1.2 m/s.[46]

4. Modeling Heat-Transfer Phenomena: Riser Side

Studies concerning heat transfer to flowing suspensions can be grouped in two categories: (a) development of empirical correlations applicable to specific solids such as FCC catalyst, graphite, and glass particles; (b) contributions leading to a better understanding of the mechanisms involved in heat transfer in flowing suspensions.

Regarding heat transfer in a gas−solid suspension, it is widely reported that the heat-transfer coefficients for a gas−solid suspension are larger than those for the gas phase alone. This increase of the heat transfer is generally attributed to the presence of solids near the walls. Boothroyd[47] proposed the following mechanisms as taking part in the heat-transfer process: (1) thinning of the boundary layer, (2) wall-contact heat transfer, and (3) reduced wall eddy diffusivity.

For the specific FCC Multicrackex unit, operating with a riser and a dense-phase fluidized-bed regenerator exchanging significant heat, one problem encountered was the lack of a heat-transfer coefficient correlation applicable to this specific design. In this respect, a number of correlations selected from the technical literature and reported in Table 1 were not able to represent the experimental results obtained in the Multicrackex unit.

Given these facts, an equation accounting for the tube Reynolds number, catalyst-to-oil ratio, and particle slip (through the term u_t/u_{gas}) was considered to represent the heat-transfer coefficient riser side of the Multicrackex unit as follows:

$$\frac{h_{riser}d_t}{\lambda_g} = \omega\left(\frac{d_tG_g}{\mu_g}\right)^{\delta}\left(\frac{F_p}{F_g}\right)^{\Phi}\left(\frac{u_t}{u_g}\right)^{\tau} \tag{4}$$

Parameters and the suitability of eq 4 were analyzed using, as will be reported later in this study, the experimental temperature profiles measured at strategic locations inside the Multicrackex unit. These parameters were also calculated by employing an advanced statistical analysis.

Table 3

a. FCC Four-Lump Model[18]

Constitutive Equations

$$\frac{dy_i}{dz} = \frac{\rho_g(1-\epsilon)AMW_i}{F_g}r_i$$

$$\frac{dC_c}{dz} = \frac{\rho_p(1-\epsilon)A\rho_g}{F_p}r_c$$

Rate Equations

Gas Oil Lump: $$-r_1 = \frac{(k_{1,2}+k_{1,3}+k_{1,4})(y_1\rho_g)^2\phi}{MW_1}$$

Gasoline Lump: $$r_2 = \frac{[k_{1,2}(y_1\rho_g)^2 - k_{2,4}y_2\rho_g - k_{2,3}y_2\rho_g]\phi}{MW_2}$$

Light Gases: $$r_3 = \frac{[k_{1,3}(y_1\rho_g)^2 + k_{2,3}y_2\rho_g]\phi}{MW_3}$$

Coke: $$r_4 = \frac{[k_{1,4}(y_1\rho_g)^2 + k_{2,4}y_2\rho_g]\phi}{MW_4}$$

with $\phi = e^{-\alpha_D C_c}$

b. Kinetic Parameters after Blasetti and de Lasa[18]

i,j	$A_{i,j}$[c]	$E_{i,j}$ (kcal/kmol)	$k_{i,j}$[c]
1,2	0.3198×10^6	19208 (±4.5%)	1.626 (±3.4%)
1,3	0.5017×10^8	28857 (±3.8%)	0.559 (±4.9%)
1,4	0.1100×10^4	13176 (±7.5%)	0.257 (±3.7%)
2,3	0.1299×10^{16}	59414 (±9.8%)	0.054 (±24.9%)
2,4	0.1422×10^7	25261 (±7.2%)	0.155 (±9.1%)
D			406.4 (±2.0%)

[a] 1 = gas oil, 2 = gasoline, 3 = light gases, 4 = coke, or simply D = for the deactivation constant. [b] Reaction rate constants and activation: i and j represent the reaction paths between the different lumps. [c] $k_{1,2}$, $k_{1,3}$, and $k_{1,4}$ are expressed in m^6/[(kg of catalyst)·kg·s]; $k_{2,3}$ and $k_{2,4}$ are expressed in m^3/[(kg of catalyst)·s]; k_D is expressed in 1/s at 793 K.

5. Modeling Heat Transfer in the Multicrackex Unit

Equation 4 was obtained by modeling the temperature profile in the section of the riser immersed in the dense phase of the regenerator.

It should be mentioned that many studies previously reported in the technical literature involve the indirect measurement of local heat-transfer coefficients through the estimation of the heat supplied to the system and a thermal balance to determine the temperature of the gas−solid suspension.

Regarding the specific methodology for the determination of the heat-transfer coefficient in the Multicrackex unit, a set of five ordinary differential equations were considered. Four of these differential equations (Table 3a) represent the mass balances for gas oil, gasoline, light gases, and coke.[18] The fifth ordinary differential equation describes the heat balance in a differential section of the riser unit and allows one to

Table 4. Comparison of Heat-Transfer Coefficients for a Number of Typical Runs in the Regenerator and Riser Sides of the Multicrackex Unit [Units: W/(m²·K)]

heat-transfer correlation	run no. 51	44	43	42	33	52	50	47	36
Heat-Transfer Correlation Proposed for the Riser (h_{riser})									
$\frac{h_{riser}d_t}{\lambda_g} = \omega\left(\frac{d_t G_g}{\mu_g}\right)^{\delta}\left(\frac{G_p}{G_{go}}\right)^{\Phi}\left(\frac{u_t}{u_g}\right)^{\tau}$	23.8	50.7	35.6	40.3	17.2	57.5	57.3	33.7	26.9
Particle Convective Component Correlations (h_{reg})									
$\frac{h_{max}d_p}{\lambda_g} = 0.134\left(\frac{\sqrt{d_p{}^3 g(\rho_p-\rho_g)^{0.6}}}{\mu_g}\right)\left(1+\frac{\lambda_g}{2C_{ps}\mu_g}\right)^{-1}$ *a*	828	827	827	823	833	837	836	839	839
$h_{max} = 35.7\rho_p{}^{0.2}\lambda_g{}^{0.6}d_p{}^{-0.36}$ *b*	730	729	730	730	735	741	740	743	744
$\frac{h_{max}d_p}{\lambda_g} = 0.75\left(\frac{d_p{}^3 g(\rho_p-\rho_g)\rho_g}{\mu_g{}^2}\right)^{0.22}\left(1-\frac{d_t}{X_t}\right)^{0.14}$ *c*	544	528	534	532	569	526	531	543	554
Radiant Component Equation									
$h_r = \frac{5.67\times10^{-8}\epsilon_r(T_b{}^4 - T_s{}^4)_d}{T_b - T_s}$	86.0	80.4	80.7	81.0	83.4	90.5	90.3	92.1	92.7

[a] References 35 and 37. [b] Reference 36. [c] Reference 38. [d] Stefan−Boltzmann's equation.

describe the temperature changes in the riser as follows:

$$\frac{dT_{riser}}{dz} = \frac{\frac{\Delta H_c F_g}{MW_0}\frac{dy_1}{dz} + \pi d_t U(T_{reg} - T_{riser})}{F_g C_{pg} + F_p C_{ps}} \quad (5)$$

Concerning the technique used for the evaluation of the overall heat-transfer coefficients of eq 5, the following was adopted: (a) Kinetic parameters were calculated first using the subset of ordinary differential equations for gas oil, gasoline, light gases, and coke (Table 3a,b), the experimentally measured temperature profile, and a nonlinear regression technique.[18] (b) Once the kinetic parameters were determined and with the C_{ps}, C_{pg}, and ΔH_c thermodynamic constants,[18] eq 5 was solved numerically using a fourth-order Runge−Kutta−Wess integration algorithm. The axial temperature profiles resulting from eq 5 were fitted to the temperatures measured at different axial positions. Heat-transfer parameters of eq 5 were simultaneously adjusted using a weighted least-squares algorithm for the estimation of nonlinear parameters.

Once the overall heat-transfer coefficient, U, was determined and considering the relationship of U with the individual heat-transfer coefficients, $U = 1/(1/h_{reg} + 1/h_{riser})$, the controlling heat-transfer step was investigated. The analysis involved the following two steps: (a) calculation of h_{reg} using eq 1; (b) given U, the calculation of h_{riser} [$h_{riser} = 1/(1/U - 1/h_{reg})$.

Regarding h_r, the reduced emissivity (ϵ_r) of the radiant component term (h_r)was calculated considering that the bed and the riser surface were two infinite parallel planes,[29] where the emissivity of the bed itself could be evaluated in a manner similar to that for a dusty gas stream.[36] For approximate calculations, recommended values of the reduced emissivity are between 0.5 and 0.6[48] and up to 0.7.[39] The reduced emissivity value selected in the present study was 0.56.

In addition, other required transport properties, such as thermal conductivity, viscosity, and density were reevaluated for each Δz increment. For instance, the thermal conductivity of the individual species was calculated using Eucken's equation[49] and the thermal conductivity of the gas mixture evaluated as follows:

$$\lambda_f = \frac{\sum_{i=1}^{N} n_i \lambda_i MW_i{}^{1/3}}{\sum_{i=1}^{N} n_i MW_i{}^{1/3}} \quad (6)$$

To overcome some difficulties encountered for the calculation of the viscosity for all of the species in the system, such values were evaluated at different temperatures by linear interpolation of viscosity values recorded at three different temperature levels.[1]

It was observed that once the radiant component was included (Table 4) h_{reg} was consistently at least 16 times larger than h_{riser}. In fact, h_{reg} ranged typically from 16 up to 40 times, when Molerus' and Zabrodsky's correlations and h_r were considered. In other words, the overall heat-transfer coefficient values, U, were close to the heat-transfer coefficient in the riser side of the Multicrackex unit.

6. Heat-Transfer Correlation and Evaluation of Parameters

Using a nonlinear least-squares algorithm, the presence of unexpected autocorrelated residuals, as shown in Figure 4, was noticed. Autocorrelated errors, which may be introduced to the experimental information when data are sequentially collected over a period of time, tend to increase the variance of the residuals. Thus, the resulting model parameters are less precise and more cross-correlated. Autocorrelation and partial autocorrelation functions (acf and pcf), reported in Figure 4b,c, show that either the proposed model was incorrect or there was a high degree of correlation between residuals.

It has been indicated[50,51] that models fitted to experimental information collected over a period of time (such as was the case of the experimental temperature profile) may show a high degree of correlation between successive error terms (residuals). The stationarity of the experimental data was secured by implementing a

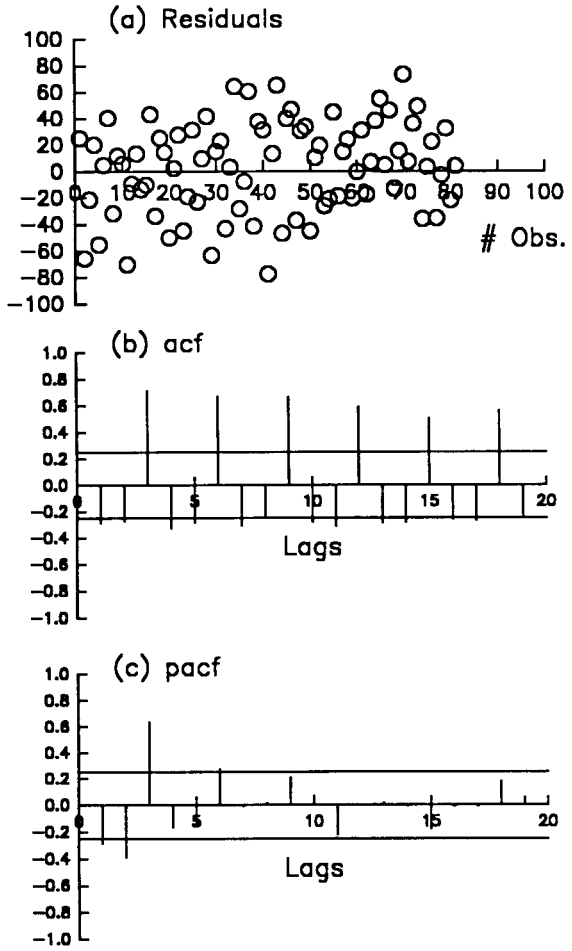

Figure 4. Analysis of residuals obtained for the proposed heat-transfer correlation after fitting of the experimental information using an unweighted nonlinear least-squares algorithm: (a) residuals versus observation number; (b) acf; (c) pacf.

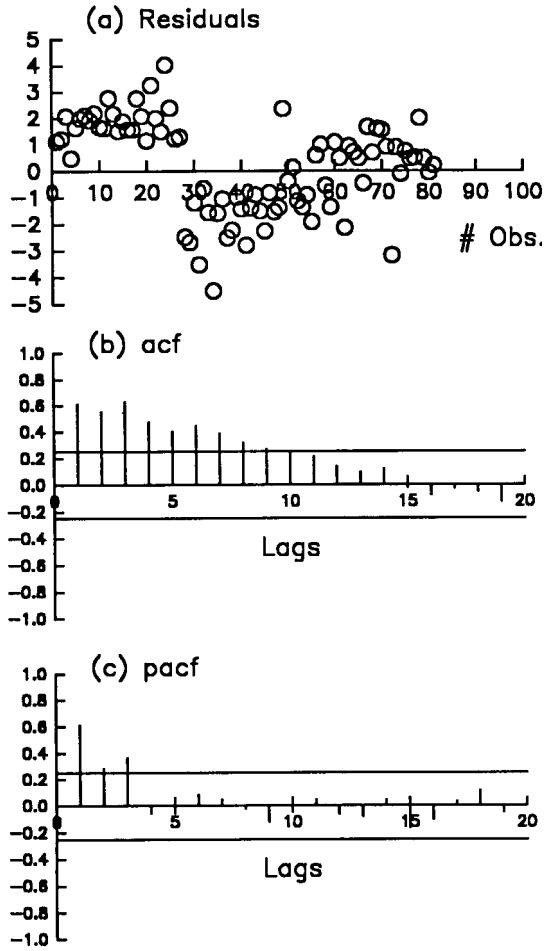

Figure 5. Analysis of residuals obtained for the proposed heat-transfer correlation after fitting of the experimental information using an unweighted nonlinear least-squares algorithm (organized by thermocouple position): (a) residuals versus observation number; (b) acf; (c) pacf.

weighted nonlinear least-squares algorithm using the sample variance information available for each experimental point. However, after the experimental information was fit and the residuals were organized according to their thermocouple position (Figure 5), a local positive correlation was still observed for the first thermocouple position, followed by a sequence of negative residuals for the second thermocouple position and so on.

The presence of serial correlation of the residuals was confirmed by means of a "two-way classification analysis" of the residuals.[52] The plot of the residuals generated by this technique showed the presence of correlation, with a pattern characterized by a series of positive values followed by a series of negative ones as in the previous case. Therefore, the parameters of the heat-transfer correlation proposed in this study were evaluated by using a conditional least-squares algorithm. This technique involved a transformation of the objective function to account for correlated disturbances that are usually represented by "autoregressive moving average" (ARMA) models.[53]

To account for this dependence between residuals, the correlation process was represented by using the analysis of autocorrelation and partial autocorrelation functions of time series, based on a set of rules indicated by Box and Jenkins.[53] By this approach, the direction and strength of the statistical relationship between observations in a single data series of residuals was measured by the acf. The effect of all observations by dealing with more than two observations at a time was measured by the pacf.

Table 5. Parameter Estimates Considered for the Representation of the Correlation among Residuals

Final Parameter Estimates, ARMA-3 Parameters			
(1) −0.1640		(2) −0.216	(3) 0.5151
Autocorrelations of Residuals			
1	0.064	2	−0.108
3	−0.187	4	0.116
5	0.120	6	−0.001
7	−0.095	8	0.047
9	0.255	10	−0.078

approximately 95% confidence limit on correlations = 0.222
standard deviation of series = 1.264
χ^2 statistic = 14.09 (10 degrees of freedom)

By application of the ARMA model building rules, a model to represent the residuals was identified. Such an analysis provided an autoregressive model of order 3 (Table 5), as follows:

$$z_t = -0.16403z_{t-1} - 0.21614z_{t-2} + 0.51511z_{t-3} + \epsilon_t \quad (7)$$

This model, considered in the conditional least-squares optimization to represent the correlation among residuals, resulted in a more complicated but, however,

Table 6. Results of Conditional Nonlinear Least-Squares Parameter Estimation for the Proposed Heat-Transfer Correlation (Gas Oil SF-135; Catalyst Akzo Octaboost 6XX Series)[a]

Parameter Estimates						
ω	δ	Φ	τ	ϕ_1	ϕ_2	ϕ_3
0.6947×10^{-2}	0.1597×10^{1}	0.6293	0.5808	-0.5912×10^{-3}	-0.2676×10^{-1}	0.5095
Individual Confidence Limits and Span (%) for Each Parameter (Linear Hypothesis)						
ω	δ	Φ	τ	ϕ_1	ϕ_2	ϕ_3
0.3135×10^{-1}	0.2269×10^{1}	0.7977	0.1204×10^{1}	0.1178×10^{-1}	-0.1423×10^{-1}	0.5233
-0.1746×10^{-1}	0.9256	0.4609	-0.4271×10^{-1}	-0.1296×10^{-1}	-0.3930×10^{-1}	0.4956
(±352.6%)	(±42.0%)	(±26.6%)	(±107.3%)			

[a] Parameter (model + residuals) values via regression and individual 95% confidence limits (81 observations, 7 parameters, 74 degrees of freedom).

Table 7. Results of Conditional Nonlinear Least-Squares Parameter Estimation for the Proposed Heat-Transfer Correlation (Gas Oil SF-135; Catalyst Akzo Octaboost 6XX Series): Correlation Coefficients[a]

Correlation Matrix							
	ω	δ	Φ	τ	ϕ_1	ϕ_2	ϕ_3
ω	1.0000						
δ	−0.9252	1.0000					
Φ	−0.1581	0.2420	1.0000				
τ	−0.4272	0.7335	0.4268	1.0000			
ϕ_1	0.1332	−0.1198	0.0531	−0.0410	1.0000		
ϕ_2	0.1164	−0.0920	−0.1973	−0.0426	0.1335	1.0000	
ϕ_3	0.1286	−0.2285	−0.2892	−0.3355	−0.2289	0.2127	1.0000

[a] Correlation between parameter estimates (81 observations, 7 parameters). Variance of residuals = 0.2547×10^{-1}, 74 degrees of freedom.

more adequate nonlinear regression model to determine the heat-transfer parameters.

The response from the system (experimental temperature profile) is given by the expression

$$y_n = f(x_n,\xi) + z_n \qquad \text{with } z_n = \epsilon_n + \sum_{i=1}^{p} \phi_i z_{n-i} \quad (8)$$

where z_n represents the correlation between observations and it was fitted by ordinary least squares. In this analysis, model parameters indicated as ξ and correlated residual parameters (ϕ_i) were simultaneously evaluated. This fitting process was performed by subtracting ϕ_i times the equation y_{n-i} from y_n.[1]

On this basis, the proposed transformed objective function to be minimized for the proposed heat-transfer correlation is the following:[1]

$$S^2(\xi,\phi_j) = \left[\sum_{k}^{Tc} \sum_{n=4}^{NT} \frac{1}{\sigma_k^2} (T_{k,n}^{obs} - \bar{T}_{k,n}^{cal})^2\right] = \text{minimum} \quad (9)$$

with

$$\bar{T}_n = T_n - \sum_{i=1}^{3} \phi_i T_{n-i} \quad (10)$$

Autoregressive parameters previously obtained for the residuals were used as initial guesses during the search for the optimal. These parameters and their corresponding correlation coefficients were presented in Tables 6 and 7, respectively. As shown in Figure 6, the plot of the residuals for the proposed heat-transfer correlation did not show any pattern of signs systematically alternating. Moreover, parts b and c of Figure 6 show autocorrelation functions of the residuals cutting off to zero after $k = 0$ lags, as is usually expected for white noise.

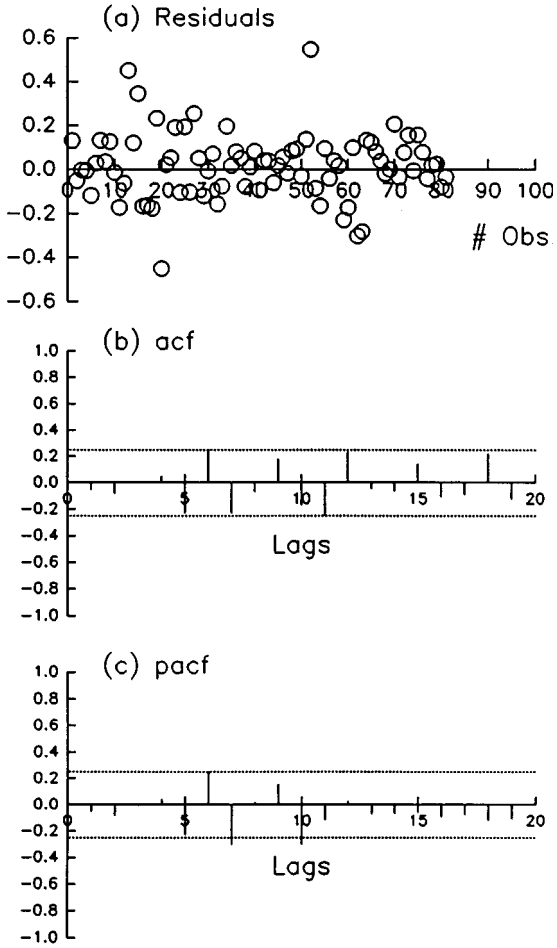

Figure 6. Analysis of residuals obtained for the proposed heat-transfer correlation after fitting of the experimental information using a conditionally weighted nonlinear least-squares algorithm: (a) residuals versus observation number; (b) acf; (c) pacf.

As reported in Table 6, two of the parameters (δ and Φ) were satisfactorily estimated, with confidence limits oscillating around ±26% and ±42%, respectively. The two other parameters, ω and τ, were, however, estimated with a relatively lower degree of precision and wider confidence limits (on linear hypothesis).

Regarding the lack of precision on ω and τ, it was attributed to the noise of the experimental data (temperature readings), which showed large local temperature variations during operation of the unit. However, this result may also be assigned to the transformation of the model, which required the introduction of ad-

ditional parameters to break the correlation of the residuals, without increasing the number of experimental observations. Therefore, additional fitting of residual parameters decreased the number of degrees of freedom and affected the precision of some of parameter estimates. Additional experimental information might reduce this unwanted effect.

Moreover and as presented in Table 7, there is little degree of correlation among parameters, with the exception of the estimates for ω and δ. This means that further improvement in the precision of some of the more imprecise parameter estimates will not significantly change the values of noncorrelated parameters.

In summary, the introduction of the parameter estimates of Table 7 and of the dimensionless numbers of eq 4 gives the following:

$$\frac{h_{\text{riser}} d_t}{\lambda_g} = 6.95 \times 10^3 \left(\frac{d_t \rho_g u_g}{\mu_g}\right)^{1.60} \left(\frac{G_p}{G_g}\right)^{0.63} \left(\frac{u_t}{u_g}\right)^{0.58} \qquad (11)$$

Concerning the characteristics of the correlation derived (eq 11), one of the most relevant aspects is that it has been developed for FCC catalyst under reaction conditions for the following range of applications: $d_T = 0.0266$ m, $L = 3.46$ m, $20 < d_p < 110$ μm (60−70 μm average), $850 < Re < 1800$, $1.2 < C/O < 12$, and $0.0195 < u_t/u_g < 0.0550$.

7. Comparison of Heat-Transfer Correlations

To test the correlation proposed, the fit between experimental versus calculated conversions and lump yield values were compared. The validity of this analysis is given by the fact that parameters for kinetic and heat-transfer models were obtained from independently evaluated experimental information. Therefore, the overall precision of the heat-transfer model could be measured in terms of prediction of conversion and selectivity.

Results of Figure 7a,b were obtained by simultaneous solution of continuity and energy equations, using the heat-transfer parameters previously estimated with eq 10 and using the simulated axial temperature profile. Lump values predicted with the combined kinetic model and heat-transfer correlation were usually found within typical error bands of 15% and 20% for the conversion and gasoline yields, respectively. Given the results reported in Figure 7a,b, it is shown that the proposed heat-transfer correlation gives a fairly good representation of the temperature and lump fractions inside the riser reactor.

However, when the same kinetic information was combined with other correlations proposed in the technical literature,[3−6] the predicted lumps did not represent well the experimentally measured lumps. For instance, it was observed that Danziger's correlation and Farbar and Morley's correlation give poor results. When the results from Danziger's correlation and Farbar and Morley's correlation are compared, it can be observed that these two correlations overpredicted both gas oil conversion and gasoline yields. Rao and Murti's equation included a larger number of dimensionless groups (Table 1). Despite this, predicted lumps with this correlation showed a similar degree of deviation than predictions obtained with Danziger's or Farbar and Morley's correlations. Finally, results from Wen and Miller's correlation (Table 1) display slightly improved

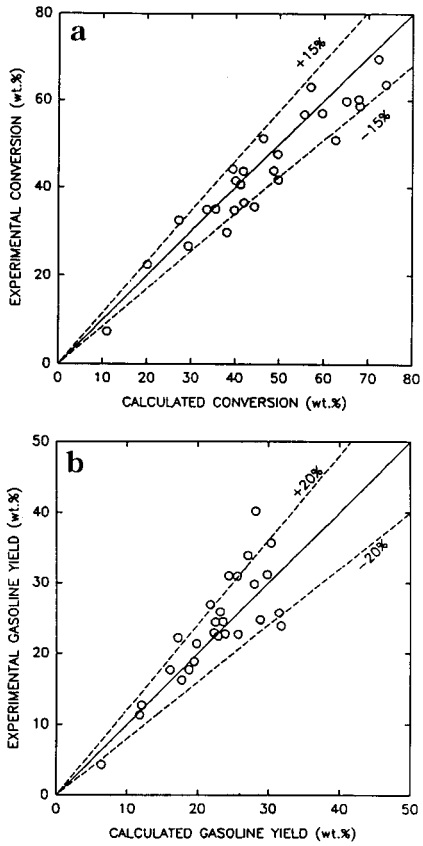

Figure 7. Comparison of (a) the experimental and calculated gas oil conversions and (b) the experimental and calculated gasoline yields using the four-lump model proposed by Blasetti and de Lasa[18] and the heat-transfer correlation of the present study.

predictions, with a tendency to overpredict the gas oil conversion and underpredict the gasoline lump.

8. Conclusions

1. The operation of the novel Multicrackex unit, constituted by a bundle of riser reactors with an upflow catalyst suspension exchanging heat with a surrounding fluidized-bed regenerator, was demonstrated at the pilot-plant scale. This design can provide a distinctive advantage for catalytic processes.

2. It is shown that the heat transfer in the Multicrackex unit is controlled by the heat-transfer rate between the gas phase/solid particle suspension in the riser side of the unit. The heat transfer in the dense fluidized bed (regenerator side) is less significant given its modest contribution to the control of the overall heat-transfer rate.

3. A statistically based correlation able to describe the heat transport phenomena between the bundle of riser reactor tubes and the fluidized-bed regenerator was developed and tested experimentally under reaction conditions for FCC units. The results of the present study are of special value for the design of novel FCC processes.

Nomenclature

A = riser cross-sectional area (m^2)
$A_{i,j}$ = i,jth preexponential factor
acp = autocorrelation function
C_c = coke concentration (kg of coke/kg of catalyst)
C_1 = dimensionless constant involved in eq 3

C_{pg} = specific heat of gases (kcal/kg·K)
C_{ps} = specific heat of catalysts (kcal/kg·K)
C/O = catalyst-to-oil ratio (kg of catalyst/kg of feedstock)
d_p = particle diameter (μm)
d_{pi} = particle diameter class i of particles (μm)
d_t = tube diameter (m)
$E_{i,j}$ = energy of activation (kcal/kmol)
g = gravity acceleration (m/s^2)
G_g = mass flow rate of gases based in the riser cross section (kg/m^2·s)
G_p = mass flow rate of particles based in the riser cross section (kg/m^2·s)
h_{reg} = heat-transfer coefficient regenerator side (W/m^2·K)
h_{pc} = particle convective component of the heat-transfer coefficient (W/m^2·K)
h_r = radiant component of the heat-transfer coefficient (W/m^2·K)
h_{riser} = heat-transfer coefficient riser side (W/m^2·K)
h_{sus} = heat-transfer coefficient in the suspension (W/m^2·K)
$k_{i,j}$ = i,jth reaction rate constant (for units refer to $k_{1,2}$, $k_{1,3}$, $k_{1,4}$, $k_{2,3}$, and $k_{2,4}$)
k_D = coke rate constant (1/s)
$k_{1,2}$ = gasoline formation rate constant in the four-lump model [m^6/(kg of catalyst)·kg·s]
$k_{1,3}$ = light gases formation rate constant in the four-lump model [m^6/(kg of catalyst)·kg·s]
$k_{1,4}$ = coke formation rate constant in the four-lump model [m^6/(kg of catalyst)·kg·s)
$k_{2,3}$ = gasoline cracking to light gases [m^3/(kg of catalyst)·s]
$k_{2,4}$ = gasoline cracking to coke [m^3/(kg of catalyst)·s]
$K_{i,\infty}$ = elutriation rate constant for size fraction d_{pi} when h >TDH (kg/m^2·s)
L = length of the riser tube (m)
MW_i = molecular weight of the ith lump (kg/kmol)
MW_o = molecular weight of the feedstock (kg/kmol)
n_i = moles of component i (kmol)
NT = number of experimental observations
Nu = Nusselt number
pacf = partial autocorrelation function
r_c = rate of coke formation [kg of coke/(kg of catalyst)·s]
r_1 = rate of reaction for gas oil in the four-lump model [kgmol/(kg of catalyst)·s]
r_2 = rate of reaction for gasoline in the four lump model [kgmol/(kg of catalyst)·s]
r_3 = rate of reaction for light gases in the four lump model [kgmol/(kg of catalyst)·s]
r_4 = rate of reaction for coke in the four lump model [kgmol/(kg of catalyst)·s]
Re = Reynolds number
S = summation of residuals
T_b = temperature of the bed (K)
Tc = variable used to represent the thermocouple number
TDH = transport disengagement height (m)
T_{ris} = riser temperature (K)
T_{reg} = regenerator temperature (K)
T_s = temperature of the riser surface (K)
$\bar{T}_n = T_n - \sum_{i=1}^{3}\phi_i T_{n-i}$
u_t = terminal velocity of a single particle (m/s)
u_g = gas superficial velocity (m/s)
U = overall heat-transfer coefficient
x_n = model variable
X_t = separation between tubes in a bundle of vertical tubes (m)
y_i = mass fraction of the ith lump, i = 1 (gas oil), i = 2 (gasoline), i = 3 (light gases), i = 4 coke (kg of i/kg of feed)
y_n, y_{n-i} = experimental measured condition, eq 7
z = axial position in the riser (m)
z_n, z_t = residuals in the heat-transfer correlation, eq 7

Greek Symbols

α_D = catalyst deactivation constant
δ = model parameter, eq 4
ΔH_c = enthalpy of cracking (kcal/kmol)
ϵ = void fraction (m^3 voids/m^3 reactor)
ϵ_n = residuals in the autoregression model, eq 7
ϵ_r = reduced emissivity
ϵ_t = residuals in the autoregression model, eq 6
ϕ = activity decay function based on coke-on-catalyst
ϕ_i = autoregression coefficients, eq 8
Φ = model parameter, eq 4
λ_g = fluid thermal conductivity (W/m·K)
μ_g = gas viscosity (cP)
ξ = model parameter, eq 8
ρ_{mix} = density of the gas−solid suspension (kg/m^3)
ρ_p = density of the catalyst particles (kg/m^3)
σ = variance
τ = correlation parameter, eq 4
ω = correlation transfer parameter, eq 4

Literature Cited

(1) Blasetti, A. P. Multitubular Reactor for FCC: Design and Kinetic Modelling. Ph.D. Dissertation, The University of Western Ontario, London, Ontario, Canada, 1994.

(2) Blasetti, A.; Ng, S.; de Lasa, H. In *Catalytic Cracking of Gas Oil in a Novel FCC Pilot Plant Unit with Heat Exchange*; Avidan, A., Ed.; Proceedings of the Circulating Fluidized Bed Conference IV, Hidden Valley Conference Center, PA, 1994; pp 458−464.

(3) Farbar, L.; Morley, M. J. Heat Transfer to Flowing Gas−Solids Mixtures in a Circular Tube. *Ind. Eng. Chem.* **1957**, *49* (7), 1143−1150.

(4) Wen, C. Y.; Miller, E. N. Heat Transfer in Solids−Gas Transport Lines. *Ind. Eng. Chem.* **1961**, *53* (1), 51−53.

(5) Danziger, W. J. Heat Transfer to Fluidized Gas−Solids Mixtures in Vertical Transport. *Ind. Eng. Chem. Process Des. Dev.* **1963**, *2* (4), 269−276.

(6) Rao, V. R. K.; Murti, P. S. Heat Transfer to Flowing Gas−Solid Suspensions in Circular Tubes. *Fluidization and Related Processes, Publications and Information Directorate*; New Delhi, India, 1966; pp 164−178.

(7) Jepson, G.; Poll, A.; Smith, W. Heat Transfer from Gas to Wall in a Gas−Solid Transport Line. *Trans. Inst. Chem. Eng.* **1963**, *41* (5), 207−211.

(8) Sukomel, A. S.; Kerimov, R. V. Methods of Generalizing Experimental Data on Heat Transfer in the Case of Turbulent Flow of a Gas Suspension in Pipes. *Heat Transfer−Sov. Res.* **1972**, *4*, 163.

(9) Yousfi, Y.; Gau, G.; Le Goff, P. Heat Transfer to an Air-Solid suspension at High Concentration and Low Velocity. *Heat Transfer* **1974**, *5*, 218−222.

(10) Matsumoto, S.; Ohnishi, S.; Maeda, S. Heat Transfer to Vertical Gas-Solid Suspension Flows. *J. Chem. Eng. Jpn.* **1978**, *11* (2), 89−95.

(11) Kim, J. M.; Seader, J. D. Heat Transfer to Gas−Solid Suspensions Flowing Cocurrently Downward in a Circular Tube. *AIChE J.* **1983**, *29* (2), 306−312.

(12) Sadek, S. E. Heat Transfer to Air−Solid Suspensions in Turbulent Flow. *Ind. Eng. Chem. Process Des. Dev.* **1972**, *11*, 133−135.

(13) Lunardelli-Furchi, J. C.; Goldstein, L.; Lombardi, G.; Mohseni, M. Heat Transfer Coefficients in Flowing Gas−Solid Suspensions. *AIChE Symp. Ser.* **1988**, *84* (263), 26−30.

(14) Muzyka, D. W. The Use of Probabilistic Multiphase Flow Equations in the Study of the Hydrodynamics and Heat Transfer in Gas−Solid Suspensions. Ph.D. Thesis Dissertation, The University of Western Ontario, London, Ontario, Canada, 1985.

(15) Bentahar, F.; Molodtsof, Y.; Large, J. F.; Alia, K. Heat Transfer to Vertically Flowing Dilute and Dense Phase Gas−Solids Suspensions. *AIChE Symp. Ser.* **1990**, *276* (86), 10−15.

(16) Kuo, J. T.; Chiou, C. H. Momentum and Heat Transfer of Gas−Solid Suspensions in Vertical Pipes. *AIChE Symp. Ser.* **1988**, *263* (84), 31−37.

(17) Knowlton, T. M. In *Gas Fludization Technology*; Geldart, D., Ed.; John Wiley: New York, 1986.

(18) Blasetti, A.; de Lasa, H. Riser Reactor with Heat Exchange in a Novel FCC Pilot Plant Unit. Kinetic Modelling. *Ind. Eng. Chem. Res.* **1997**, *36*, 3223−3229.

(19) Botterill, J. S. M. *Fluid-Bed Heat Transfer*; Academic Press: London, 1975.

(20) Botterill, J. S. M. Fluid Bed Heat Transfer. In *Gas Fluidization Technology*, Geldart, D., Ed.; John Wiley: New York, 1986.

(21) Flamant, G.; Fatah, N.; Flitris, N. Wall-to-Bed Heat Transfer in Gas−Solid Fluidized Beds: Prediction of Heat Transfer Regimes. *Powder Technol.* **1992**, *69*, 223−230.

(22) Lu, J. D.; Flamant, G.; Snabre, P. Towards a Generalized Model for Vertical Walls to Gas−Solid Fluidized Beds Heat Transfer−I. Particle Convection and Gas Convection. *Chem. Eng. Sci.* **1993**, *48* (13), 2479−2492.

(23) Figliola, R. S.; Beasley, D. E. A Study of the Particle Convection Contribution to Heat Transfer in Gas Fluidized Beds. *Chem. Eng. Sci.* **1993**, *48* (16), 2901−2911.

(24) Mazza, G. D.; Barreto, G. F. Analysis of Models for Heat Transfer Between Gas-Fluidized Beds and Immersed Surfaces at High Temperatures. *Powder Technol.* **1993**, *75*, 173−179.

(25) Adams, R. L.; Welty, J. R. A Gas Convective Model of Heat Transfer in Large Particle Fluidized Bed. *AIChE J.* **1979**, *25*, 395−405.

(26) Decker, N. A.; Glicksman, L. R. Heat Transfer in Large Particle Fluidized Beds. *Int. J. Heat Mass Transfer* **1983**, *26*, 1307−1320.

(27) Mazza, G. D.; Barreto, G. F. The Gas Contribution to Heat Transfer Between Fluidized Beds of Large Particles and Immersed Surfaces. *Int. J. Heat Mass Transfer* **1988**, *31*, 603−614.

(28) Lu, J. D.; Qian, R. Z. A Modelling Study to the Heat Transfer Between Immersed Surfaces and Large-Particle Fluidized Beds. *Int. J. Heat Mass Transfer* **1989**, *32*, 2375−2384.

(29) Ackeskog, H. B. R.; Almstedt, A. E.; Zakkay, V. An Investigation of Fluidized-Bed Scaling: Heat Transfer Measurements in a Pressurized Fluidized-Bed Combustor and a Cold Model. *Chem. Eng. Sci.* **1993**, *48* (8), 1459−1473.

(30) Mickley, H. S.; Fairbanks, D. F. Mechanism of Heat Transfer to Fluidized Beds. *AIChE J.* **1955**, *1*, 374−384.

(31) Botterill, J. S. M.; Williams, J. R. The Mechanism of Heat Transfer in Gas Fluidized Beds. *Trans. Inst. Chem. Eng.* **1963**, *41*, 217−230.

(32) Koppel, L. B.; Patel, R. D.; Holmes, J. T. Wall to Fluidized Bed Heat Transfer Coefficients: Part IV. *AIChE J.* **1970**, *16*, 464−471.

(33) Zabrodsky, S. S.; Epanov, Y. G.; Galershtein, D. M.; Saxena, S. C.; Kolar, A. K. Heat Transfer in a Large-Particle Fluidized Bed with Immersed in-line and Staggered Bundles of Horizontal Smooth Tubes. *Int. J. Heat Mass Transfer* **1981**, *24* (4), 571−579.

(34) Xavier, A. M.; Davidson, J. F. Heat Transfer in Fluidized Beds: Convective Heat Transfer in Fluidized Beds. In *Fluidization*, 2nd ed.; Davidson, J. F., Clift, R., Harrison, D., Eds.; Academic Press: London, 1985; p 437.

(35) Molerus, O. Heat Transfer in Gas Fluidized Beds−Part 1. *Powder Technol.* **1992**, *70*, 1−14.

(36) Zabrodsky, S. S. Hydrodynamics and Heat Transfer in Fluidized Beds, Chapter 10, 226−300. The Massachusetts Institute of Technology Press, 1966.

(37) Molerus, O. Heat Transfer in Gas Fluidized Beds−Part 2: Dependence of Heat Transfer on Gas Velocity. *Powder Technol.* **1992**, *70*, 15−20.

(38) Gelperin, N. I.; Einstein, V. G. Heat Transfer in Fluidized Beds. In *Fluidization*; Davidson, J. F., Harrison, D., Eds.; Academic Press: London, 1971; Chapter 10, p 471.

(39) Gabor, J. D.; Botterill, J. S. Heat Transfer in Fluidized and Packed Beds. In *Handbook of Heat Transfer Applications*; Roshenow, W. M., Hartnett, J. P., Ganic, E. N., Eds.; McGraw-Hill Book Company: New York, 1985.

(40) Grace, J. R. Heat Transfer in Circulating Fluidized Beds. In *Circulating Fluidized Bed Technology*; Basu, P., Large, J. F., Eds.; Pergamon Press: Oxford, U.K., 1986; p 13.

(41) Mahalingam, M.; Kolar, A. K. Emulsion Layer Model for Wall Heat Transfer in a Circulating Fluidized Bed. *AIChE J.* **1991**, *37* (8), 1139−1150.

(42) Basu, P.; Nag, P. K. An Investigation into Heat Transfer in circulating Fluidized Beds. *Int. J. Heat Mass Transfer* **1987**, *30* (11), 2399−2409.

(43) Subbarao, D.; Basu, P. A Model for Heat Transfer in Circulating Fluidized Beds. *Int. J. Heat Mass Transfer* **1986**, *29* (3), 487−489.

(44) Hashimoto, O.; Mori, S.; Hiraoka, S.; Yamada, I.; Kojima, T.; Tsuji, K. Heat Transfer to the Surface of Vertical Tubes in the Freeboard of the Turbulent Fluidized Bed. *Kagaku Kogaku Ronbunshu* **1988**, *14* (3), 267−271.

(45) Zenz, F. A.; Weil, N. A. Theoretical−Empirical Approach to the Mechanism of Particle Entrainment from Fluidized Beds. *AIChE J.* **1958**, *4*, 472−479.

(46) Geldart, D. In *Gas Fluidization Technology*; Geldart, D., Ed.; John Wiley & Sons: New York, 1986.

(47) Boothroyd, R. G. *Heat Transfer in Flowing Gas−Solids Suspensions*; Chapman and Hall Ltd.: London, 1971.

(48) Baskakov, A. P.; Filippovsky, N. P. A Simple Method of Heat Transfer Calculations in fluidized Bed Furnaces. In *Fluidization VI*; Grace, J. R., Schmidt, W., Bergougnou, M. A., Eds.; Engineering Foundation: Banff, Alberta, 1989; pp 695−700.

(49) Reid, R.; Prausnitz, J.; Sherwood, T. *The Properties of Gases and Liquids*, 3rd ed.; McGraw-Hill: New York, 1977.

(50) Draper, N.; Smith, H. *Applied Regression Analysis*, 2nd ed.; John Wiley and Sons: New York, 1981.

(51) Seber, G. A. F.; Wild, C. J. *Nonlinear Regression*; John Wiley and Sons: New York, 1989.

(52) Anscombe, F. J.; Tukey, J. H. The Examination and Analysis of Residuals. *Technometrics* **1963**, *5* (2), 141.

(53) Box, G. E. P.; Jenkins, G. M. *Time Series Analysis: Forecasting and Control*; Holden-Day Inc.: San Francisco, CA, 1976.

Received for review October 13, 2000
Revised manuscript received June 20, 2001
Accepted July 23, 2001

IE0008777